Molecular Dynamics Study on Incorporating Electronic Excitation in Machine Learning Potentials for Improved Phase Stability of Beta-U

Jae-Hyuk Kim a and Takuji Oda a*

^aDepartment of Energy System and Engineering, Seoul National University, 1 Gwanak-ro, Gwanak-gu, Seoul, 08826, Republic of Korea

*Corresponding author: oda@snu.ac.kr

*Keywords: metallic uranium, molecular dynamics, moment tensor potential, first-principles calculation

1. Introduction

Despite its crucial role alongside other crystallographic phases of uranium in assessing radiation damage behavior of metallic uranium fuels designed for advanced sodium fast reactors (SFRs), reliable reproduction of β -U (tetragonal, $P4\nu/mnm$) in molecular dynamics (MD) simulations remains a significant challenge [1], [2], [3], [4]. Accurate representation of β -U, as with other phases, is essential for predicting key radiation damage properties, including radiation-induced defect formation, defect distribution, and the resulting changes in mechanical and thermal properties.

In our recent work [5], we developed a machine learning interatomic potential within the moment tensor potential (MTP) framework [6] that incorporates all uranium explicitly experimentally identified at ambient pressure: α-U (orthorhombic, CmCm), β -U, γ -U (cubic, $Im\overline{3}n$), and liquid-U [7]. Consistent with earlier reports, however, our baseline potential (hereafter MTP_{main}) exhibited pronounced instability of β-U and failed to capture its phase transformations from other phase [1], [2], [3], [4], [5]. Complementary density functional theory (DFT) calculations quantitatively revealed that the inclusion of electronic excitation effects, already recognized as crucial for γ-U at elevated temperatures [9], also improves the relative phase stability of β -U with respect α-U. Nevertheless, reproduction of transformations from other phases remained elusive. [5].

Previous attempts to address electronic excitation in MTPs have commonly adopted a phasespecific strategies, in which independent MTPs are built for each phase of uranium [10], [11]. While this approach successfully incorporated the electronic excitation, it has two major drawbacks to be used as baseline MTP for radiation damage simulation for SFR assessments: substantially (i) increased computational cost, since every training configuration requires explicit DFT calculations with electronic excitation effects, and (ii) lack of information in β -U as it was proposed for high-temperature and high-pressure region outside of interest of SFR. As an alternative to previous approaches, the present study introduces an auxiliary potential, denoted MTPee, designed to capture the electronic excitation effects in a phase-universal

manner. This strategy not only provides the essential stabilization mechanism of β -U while also eliminates the need for multiple phase-specific potentials, thereby assuring better physical description on metallic uranium and improving computational efficiency.

2. Methods

In this section, we describe the construction and implementation of the auxiliary potential (MTP $_{ee}$) in MD simulations, together with the methodology used to evaluate its effect on stabilizing β -U. All MD simulations were carried out using the Large-scale Atomic/Molecular Massively Parallel Simulator (LAMMPS) [12], and all DFT calculations were performed with the Vienna Ab-initio Simulation Package (VASP) [13].

2.1 Construction of Auxiliary Potential (MTP_{ee})

The key distinction of our approach from previous MTPs incorporating electronic excitation lies in separating energy contributions rather than constructing phase-specific potentials. In particular, the vibrational term is described by MTP_{main} , while the contribution from electronic excitation is captured exclusively by MTP_{ee} .

To train MTP $_{ee}$, we selected a representative subset of configurations from the full dataset previously used for MTP $_{main}$. For these configurations, DFT calculations were performed using the Fermi-Dirac smearing method with a smearing width of σ =k $_B$ T (eV), thereby accounting for the electronic excitation effects. The electronic excitation contribution to energy, forces, and stresses was obtained by subtracting the corresponding quantities obtained in our earlier study without electronic excitation from those obtained using Fermi-Dirac smearing. This resulting dataset was then employed to train MTP $_{ee}$ with the same hyperparameters applied for MTP $_{main}$ [5].

Although using multiple smearing widths would enrich the training set by covering excitation effects across various temperatures, the computational cost of such calculations is substantially high. Therefore, in the present study, we carried out Fermi-Dirac smearing calculations only at 1000 K. The extension of

MTP_{ee} to other temperatures is discussed in the following section.

2.2 Hybridization with Baseline MTP

Classical MD simulations inherently lack the degrees of freedom to dynamically capture electronic excitation effects. To overcome this limitation, we hybridized MTP $_{\rm ee}$ with MTP $_{\rm main}$, introducing an additional temperature-dependent scaling factor. Since MTP $_{\rm ee}$ was trained specifically at 1000K, scaling is required to generalize its applicability to other temperatures.

To determine this scaling factor, static DFT calculations were performed for $\alpha\text{-}$ and $\beta\text{-}U$ using equilibrium lattice constants obtained at 1000 K from the hybridized potential. Different smearing widths were applied to extract the electronic excitation energies at various temperatures. Corresponding static calculations were then carried out using MTP_{ee}, and the ratio of excitation energies between DFT and MTP_{ee} was defined as a phase- and temperature-dependent scaling factors.

To validate the hybridization, we evaluated the lattice thermal expansion and enthalpy of each phase and compared the results with those from MTP_{main} with DFT corrections and experimental data [5], [14]. MD simulations were performed for systems containing more than 10,000 atoms under the NPT ensemble across a range of temperatures. After sufficient equilibration, average lattice constants were obtained. Subsequent NVT simulations at these lattice constants were then used to extract atomic enthalpies of each phase.

2.3 Evaluation of Relative Stability via Gibbs Free Energy

The nonequilibrium thermodynamic integration (NETI) method provides a robust and accurate means of calculating free energy differences by gradually transforming one system into another through a parameterized Hamiltonian path [15]. The free energy difference ΔF between two states, typically the system of interest and the reference state (e.g., an Einstein crystal for solids), is obtained by integrating the average work performed during nonequilibrium switching simulations connecting the initial and final states.

In this study, NETI was employed to evaluate the relative stability of $\beta\text{-U}$ with respect to $\alpha\text{-U}$ using both hybridized MTP and MTP alone. This analysis highlights the advantage of our framework: unlike

previous MTPs, which cannot separate vibrational and electronic excitation contributions, our method allows such decomposition, thereby enabling a more transparent free-energy analysis [10], [11].

To reduce computational cost, NETI simulations were performed at a single reference temperature for both phases. The temperature dependence of Gibbs energy was subsequently derived using enthalpy data obtained in Section 2.2, rather than repeating NETI across multiple temperatures.

3. Results and Discussion

3.1 Thermodynamic Properties using the Hybridized MTPs

The lattice thermal expansion of $\alpha\text{-}$ and $\beta\text{-}U$ obtained from MTP_main, the hybridized potential, and experimental data is shown in Figure 1. For both phases, the inclusion of electronic excitation leads to an increase in the predicted volume, particularly for $\beta\text{-}U$ at elevated temperatures. The hybridized potential provides a slightly better approximation to experiment than MTP_main alone, indicating an improved description of temperature-dependent structural behavior.

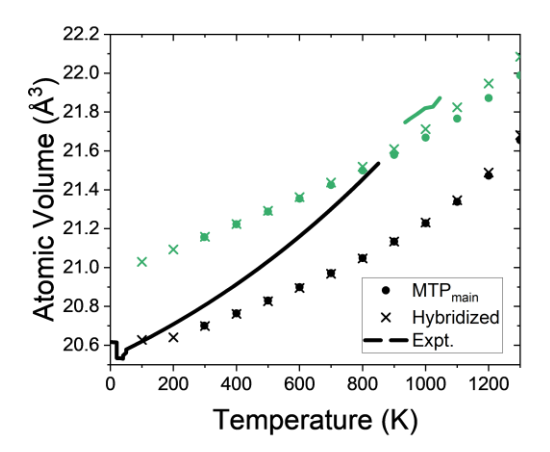


Figure 1. Comparison of lattice thermal expansion in α -(black symbols and solid line) and β -U (green symbols and solid line).

To further verify the hybridization, the enthalpies of α -and β -U were evaluated at various temperatures and are presented in Figure 2. The hybridized potential successfully reproduces the expected enthalpy increase due to electronic excitation derived from DFT with less than 1 meV/atom deviation, thereby validating the hybridization framework.

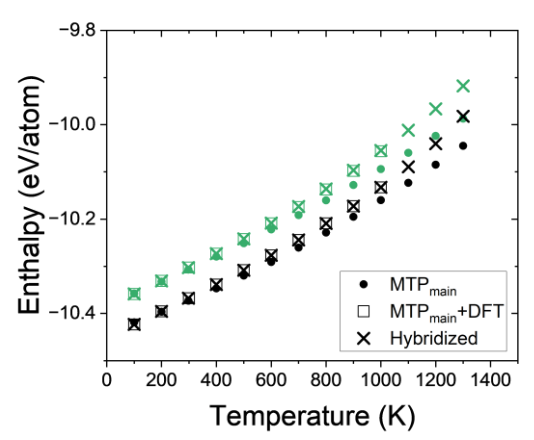


Figure 2. Comparison of enthalpy in α - (black symbols) and β -U (green symbols).

Subsequently, comparison with experimental enthalpies is given in Figure 3, where the relative enthalpy of α -and β -U is referenced to α -U at room temperature. While some discrepancies remain, the hybridized potential demonstrates improved agreement with the experiment than MTP_main alone. Taken together, the lattice thermal expansion and enthalpy analyses confirm that incorporating electronic excitation via the hybrid approach is valid.

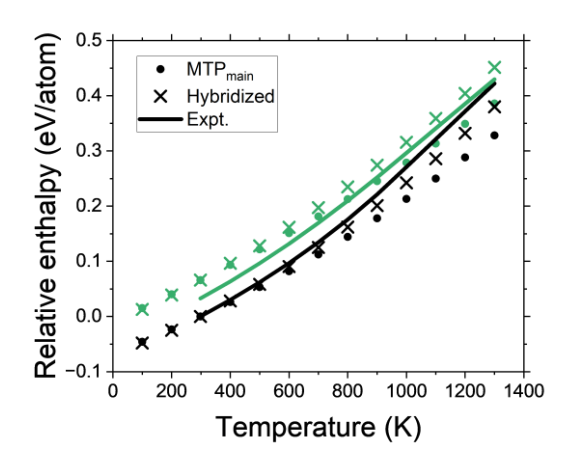


Figure 3. Relative enthalpy of α - (black symbols) and β - U (green symbols) referenced to α -U at room temperature.

3.2. Gibbs Energy Comparison

The relative Gibbs free energy of β -U with respect to α -U, calculated using MTP_{main}, MTP_{main} with DFT-based corrections, and hybridized potential, are shown in Figure 4 and compared with experiments. Incorporating electronic excitations causes a substantial downward shift in the free energy of β -U across the entire temperature range, resulting in a reduction in more than 200 K in the $\alpha \rightarrow \beta$ crossover temperature compared to MTP_{main} (1542 K \rightarrow 1324 K). The relative free energies obtained calculated using the NETI

method with MTP $_{main}$ and DFT-based corrections predict the α - β crossover at approximately 1200 K; however, this temperature is not fully reproduced by the hybridized potential. This discrepancy is thought to arise from the dynamic effects on phase stability that are captured in MD simulations with the hybridized potential, but not included in static DFT corrections.

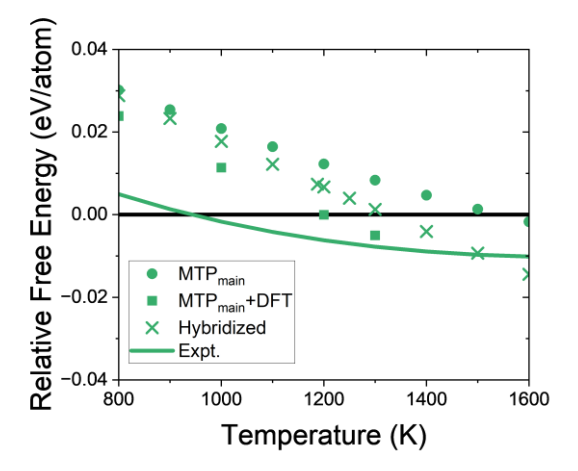


Figure 4. Relative free energy of β -U with respect to α -U calculated from MTP_{main} alone, MTP_{main} with DFT-based corrections, and hybridized potential compared with experiments.

Since previous MTPs were developed in a phase-specific manner, considering the electronic excitation from the initial stage of potential construction, and did not include β -U but instead a different phase of γ '-U (tetragonal, *14/mmm*), the presented hybridized MTP is expected to be more efficient in terms of computational cost and widely used as a baseline potential for various simulations interested in the phases relevant to SFR operation, such as radiation damage and defect evolution studies.

Meanwhile, there is still a significant discrepancy between experimental data and the hybridized potential results in Figure 4. This difference is expected to stem primarily from the DFT exchange-correlation functional, and finding a superior one remains a challenge for accurately simulating uranium.

4. Conclusions

In this study, we introduced a hybrid machine-learning potential framework to investigate the effect of electronic excitation on the phase stability of $\beta\text{-U}$. The approach separates the vibrational and electronic excitation contributions, with MTP $_{main}$ describing lattice vibrations and MTP $_{ee}$ accounting for electronic excitation in a phase-universal manner.

The validity of this framework was demonstrated through systematic comparisons against experimental data and DFT-based corrections. The hybrid potential reproduced key thermodynamic properties, including lattice thermal expansion and enthalpy, with improved

accuracy relative to MTP_{main} alone. Most importantly, the inclusion of electronic excitation led to a stabilization of β -U, indicated by a downward shift of more than 200 K in the $\alpha \rightarrow \beta$ transformation temperature. This stabilization was not fully consistent with the DFT-corrected predictions, probably due to the dynamic effects that are captured in MD simulations with the hybridized potential, but not included in static DFT corrections. Beyond methodological significance, the proposed hybridized potential is specifically designed to cover uranium phases that are important in SFR metallic fuels. We anticipate that our hybridized MTPs will serve as an effective baseline potential for radiation damage simulations aimed at calculating key radiation-induced properties for phases of uranium related to the operational and accident temperature and pressure conditions of SFR.

ACKNOWLEDGMENTS

This research was supported by the National Research Foundation of Korea (NRF) grant funded by the Korea government (MSIT) (RS-2024-00436693).

REFERENCES

- [1] M. I. Pascuet, G. Bonny, and J. R. Fernández, "Many-body interatomic U and Al–U potentials," *J. Nucl. Mater.*, vol. 424, no. 1–3, pp. 158–163, May 2012, doi: 10.1016/J.JNUCMAT.2012.03.002.
- [2] D. E. Smirnova, S. V Starikov, and V. V Stegailov, "Interatomic potential for uranium in a wide range of pressures and temperatures," *J. Phys. Condens. Matter*, vol. 24, no. 1, p. 015702, Jan. 2012, doi: 10.1088/0953-8984/24/1/015702.
- [3] J. R. Fernández and M. I. Pascuet, "On the accurate description of uranium metallic phases: a MEAM interatomic potential approach," *Model. Simul. Mater. Sci. Eng.*, vol. 22, no. 5, p. 055019, Jul. 2014, doi: 10.1088/0965-0393/22/5/055019.
- [4] H. Chen, D. Yuan, H. Geng, W. Hu, and B. Huang, "Development of a machine-learning interatomic potential for uranium under the moment tensor potential framework," *Comput. Mater. Sci.*, vol. 229, p. 112376, Oct. 2023, doi: 10.1016/J.COMMATSCI.2023.112376.
- [5] J.-H. Kim and T. Oda, publication under preparation
- [6] A. V Shapeev, "MOMENT TENSOR POTENTIALS: A CLASS OF SYSTEMATICALLY IMPROVABLE INTERATOMIC POTENTIALS *," vol. 14, no. 3, pp. 1153–1173, doi: 10.1137/15M1054183.
- [7] C.-S. Yoo, H. Cynn, and P. Söderlind, "Phase diagram of uranium at high pressures and temperatures," *Phys. Rev. B*, vol. 57, no. 17, pp. 10359–10362, 1998, doi: 10.1103/PhysRevB.57.10359.
- [8] H. Chen, D. Yuan, H. Geng, W. Hu, and B. Huang, "Development of a machine-learning interatomic potential for uranium under the moment tensor potential framework," *Comput. Mater. Sci.*, vol. 229,

- p. 112376, Oct. 2023, doi: 10.1016/J.COMMATSCI.2023.112376.
- [9] P. Söderlind, A. Landa, E. E. Moore, A. Perron, J. Roehling, and J. T. McKeown, "High-Temperature Thermodynamics of Uranium from Ab Initio Modeling," *Appl. Sci.*, vol. 13, no. 4, p. 2123, Feb. 2023, doi: 10.3390/app13042123.
- [10] I. A. Kruglov, A. Yanilkin, A. R. Oganov, and P. Korotaev, "Phase diagram of uranium from ab initio calculations and machine learning," *Phys. Rev. B*, vol. 100, no. 17, p. 174104, Nov. 2019, doi: 10.1103/PhysRevB.100.174104.
- [11] P. V. Chirkov, G. S. Eltsov, R. M. Kichigin, A. A. Mirzoev, A. V. Karavaev, and V. V. Dremov, "Machine learning enhanced quantum molecular dynamics assessment of the phase diagram of uranium," *Phys. Rev. B*, vol. 112, no. 2, p. 024104, Jul. 2025, doi: 10.1103/8w5w-f3kd.
- [12] A. P. Thompson *et al.*, "LAMMPS a flexible simulation tool for particle-based materials modeling at the atomic, mes o, and continuum scales," *Comput. Phys. Commun.*, vol. 271, p. 108171, Feb. 2022, doi: 10.1016/J.CPC.2021.108171.
- [13] G. Kresse and J. Furthmüller, "Efficient iterative schemes for ab initio total-energy calculations using a plane-wave basis set," *Phys. Rev. B*, vol. 54, no. 16, pp. 11169–11186, Oct. 1996, doi: 10.1103/PhysRevB.54.11169.
- [14] A. T. Dinsdale, "SGTE data for pure elements," Calphad, vol. 15, no. 4, pp. 317–425, 1991, doi: 10.1016/0364-5916(91)90030-N.
- [15] R. Freitas, M. Asta, and M. De Koning, "Nonequilibrium free-energy calculation of solids using LAMMPS," *Comput. Mater. Sci.*, vol. 112, pp. 333–341, Feb. 2016, doi: 10.1016/J.COMMATSCI.2015.10.050.